AIChE

Networks with Large Solvent Recycle: Dynamics, Hierarchical Control, and a Biorefinery Application

Sujit S. Jogwar, Ana I. Torres, and Prodromos Daoutidis
Dept. of Chemical Engineering and Materials Science, University of Minnesota, Minneapolis, MN 55455

DOI 10.1002/aic.12708
Published online July 22, 2011 in Wiley Online Library (wileyonlinelibrary.com).

A class of networks featuring large recycle of solvent is analyzed. This feature is central to numerous integrated processes which use solvents in various reaction and separation steps. A prototype network capturing the essential features of such networks is identified. Rigorous dynamic analysis reveals the presence of two time-scale dynamics exhibited by this prototype network. A systematic framework for model reduction and a subsequent hierarchical control design is proposed. The advantages of the proposed design over direct model-based control are demonstrated via a simulation case study. Finally, the application of the proposed framework to a newly proposed process for the production of 5-hydroxymethylfurfural from fructose is also presented. © 2011 American Institute of Chemical Engineers AIChE J, 58: 1764–1777, 2012
Keywords: process control, multiscale modeling, large solvent recycle

Introduction

Solvent recovery and recycle, motivated by the significant cost benefits resulting from the reduced consumption of make-up solvent and the environmental regulations demanding minimal discharge of toxic chemicals, is one of the essential features of integrated chemical processes. Nonaqueous solvents are used quite often as a reaction medium with the solvent recovered and recycled back to the reactor upon separation from the product. For example, organic solvents (alkanes, ethers, etc) are used for enzyme-catalyzed processes to allow for easier product and enzyme recovery,[1–4] whereas ionic liquids-based processes have gained significant attention in recent years as they offer environmental safety and enhanced solvent recovery.[5–8] Solvents are also commonly used to purify a product of interest or to remove contaminants from waste streams. For example, phenol removal from industrial wastewater via adsorption on activated carbon uses organic solvents (e.g., acetone, *n*-pentane) to extract the adsorbed phenol during the adsorbent regeneration step;[9,10] butane is used as a solvent for extractive crystallization to achieve complete separation of xylenes beyond the eutectic composition.[11] Solvent extraction is also used to remove an important reaction intermediate, thus blocking its subsequent reactions. For example, the production of 5-hydroxymethylfurfural (HMF), an important platform chemical for biorefinery applications, using biphasic systems uses this strategy.[12] Several contributions have addressed the design and control of specific solvent recycle systems. For example, a number of (linear/nonlinear model-based) control strategies have been proposed for wastewater treatment systems,[13] whereas the design and control of extractive distillation systems (which feature recycle of solvent) has been addressed within a multiloop linear control framework.[14–16] Most of the above systems feature a large solvent recycle flow compared to fresh solvent feed flow.

In previous work,[17,22] we have demonstrated that networks featuring flows of different orders of magnitude give rise to multitime-scale dynamics which have crucial control implications. In a different vein, the control of (more general) process networks has recently attracted increased attention in the literature.[17–21] In this article, we identify the defining characteristics of processes with significant solvent recycle and incorporate them in a prototype network. We document that the material balance model of the prototype network with large solvent recycle can be recast in a singularly perturbed form similar to the one introduced for networks with large recycle of unconverted reactants.[22] We describe a model reduction framework for deriving reduced order fast and slow models of the network dynamics and highlight features of these models that are unique to the case of large solvent recycle. We also propose a hierarchical control design procedure for these networks and illustrate its advantages over direct model-based control. Finally, we focus on a recently proposed continuous process for the production of HMF which features a complex, multiloop recycle structure. We illustrate the application of the proposed controller design framework and develop a "plant-wide" control strategy for this process.

Prototype Network with Large Solvent Recycle

Figure 1 represents a prototype network with large solvent recycle. The network consists of N process units,

Correspondence concerning this article should be addressed to P. Daoutidis at daout001@umn.edu.

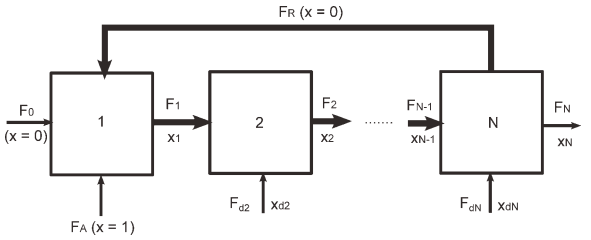

Figure 1. Prototype network with large solvent recycle.

wherein pure solute (F_A) and pure solvent (F_0) enter the first unit and the product of interest leaves through the Nth unit. The solvent is recovered in the Nth unit and is recycled back to the first unit with flowrate F_R. F_i represents the effluent flow from the ith unit and x_i represents the solute concentration in the ith unit. F_N represents the (relatively pure) product flow with solute concentration x_N. F_{d_i} represent possible additional flows (e.g., extra solute/solvent streams) to each unit, accounting for the interaction of the solvent recycle network with the rest of the plant. Owing to the fact that most solvent recycle networks involve a negligible amount of solute in the solvent recycle stream, it is assumed that the recycle flow consists of pure solvent, that is, $x_R = 0$ (this assumption can be relaxed as discussed in Remark 3).

The dynamic equations governing the overall and the component material balance for this network are

$$\begin{aligned}
&\frac{dM_1}{dt} = F_0 + F_A + F_R - F_1\\
&\frac{dx_1}{dt} = \frac{1}{M_1}[F_A(1-x_1) - (F_0+F_R)x_1 - \mathcal{R}_1(x_1)]\\
&\frac{dM_i}{dt} = F_{i-1} + F_{d_i} - F_i \qquad \text{for } i = 2,\ldots,(N-1)\\
&\frac{dx_i}{dt} = \frac{1}{M_i}\left[F_{i-1}(x_{i-1}-x_i) + F_{d_i}(x_{d,i}-x_i) - \mathcal{R}_i(x_i)\right]\\
&\frac{dM_N}{dt} = F_{N-1} + F_{d_N} - F_N - F_R\\
&\frac{dx_N}{dt} = \frac{1}{M_N}\left[F_{N-1}x_{N-1} + F_R x_N + F_{d_N}(x_{d,N}-x_N) - \mathcal{R}_N(x_N)\right]
\end{aligned} \tag{1}$$

with M_i being the holdup of the ith process unit. $\mathcal{R}_i(x_i)$ represents the rate of consumption of the solute via reaction in the ith unit.

We consider the case where the solvent recycle flow (F_R) is large compared to the fresh solvent flow (F_0). We can then define a small parameter ε as the ratio of the fresh solvent flow to the solvent recycle flow, that is

$$\frac{F_{0,s}}{F_{R,s}} = \varepsilon \ll 1$$

where the subscript s represents a steady state value. The internal material flows (F_i) are comparable in magnitude to the recycle flow and hence are also large. It is also assumed that the inlet solute flow (F_A) and the rates of consumption of the solute ($\mathcal{R}_i(x_i)$) are of the same order of magnitude as the fresh solvent flow, resulting in dilute conditions in all but the last unit, which is typically the case in such systems. This also implies that the product flow is small compared to the recycle flow. Finally, we assume that the external flows F_{d_i} are also small in comparison with the recycle flow, which is consistent with the assumption of tight integration through solvent recycle.

Based on these order of magnitude arguments, we can define $\mathcal{O}(1)$ steady state ratios k_j as

$$k_j = \begin{cases} \dfrac{F_{j,s}}{F_{0,s}} & \text{for } j = A, N, d_2, d_3, \ldots, d_N \\ \dfrac{F_{j,s}}{F_{R,s}} & \text{for } j = 1,2,3,\ldots,N-1 \end{cases}$$

and scaled material flows u_j as

$$u_j = \frac{F_j}{F_{j,s}}$$

where $j = 1,\ldots,N,A,d_2,\ldots,d_N$. Furthermore, the following $\mathcal{O}(1)$ scaled flows corresponding to the reaction rates are also defined

$$\psi_j = \frac{\mathcal{R}_j(x_j)}{F_{0,s}} \qquad \text{for } j = 1,2,3,\ldots,N-1$$

The dynamic equations in 1 can now be cast in the singularly perturbed form

$$\frac{d\mathbf{x}}{dt} = \mathbf{f}(\mathbf{x}) + \mathbf{g}_s(\mathbf{x})\mathbf{u}_s + \frac{1}{\varepsilon}\mathbf{g}_l(\mathbf{x})\mathbf{u}_l \tag{2}$$

with

$$\mathbf{x} = [M_1 \;\; x_1 \;\; \ldots \;\; M_N \;\; x_N]^T$$
$$\mathbf{u}_s = [u_0 \;\; u_A]^T$$
$$\mathbf{u}_l = [u_1 \;\; \ldots \;\; u_{N-1} \;\; u_R]^T$$

$$\mathbf{f}(\mathbf{x}) = F_{0,s}\begin{bmatrix} 0 \\ -\frac{\psi_1}{M_1} \\ k_{d,2}u_{d,2} \\ \frac{k_{d,2}u_{d,2}(x_{d,2}-x_2)-\psi_2}{M_2} \\ \vdots \\ k_{d,i}u_{d,i} \\ \frac{k_{d,i}u_{d,i}(x_{d,2}-x_i)-\psi_i}{M_i} \\ \vdots \\ k_{d,N-1}u_{d,N-1} \\ \frac{k_{d,N-1}u_{d,N-1}(x_{d,N-1}-x_{N-1})-\psi_{N-1}}{M_{N-1}} \\ k_{d,N}u_{d,N} - k_N u_N \\ \frac{k_{d,N}u_{d,N}(x_{d,N}-x_N)-\psi_N}{M_N} \end{bmatrix}$$

$$\mathbf{g}_s(\mathbf{x}) = F_{0,s}\begin{bmatrix} 1 & k_A \\ -\frac{x_1}{M_1} & \frac{k_A(1-x_1)}{M_1} \\ 0 & 0 \\ \vdots & \vdots \\ 0 & 0 \end{bmatrix}$$

$$\mathbf{g}_l(\mathbf{x}) = F_{0,\mathrm{s}} \begin{bmatrix} -k_1 & 0 & & \cdots & 0 & 1 \\ 0 & 0 & & \cdots & 0 & -\frac{x_1}{M_1} \\ k_1 & -k_2 & & & & 0 \\ \frac{k_1(x_1-x_2)}{M_2} & 0 & & & & \\ 0 & \ddots & & & & \vdots \\ & & k_{i-1} & -k_i & & \\ \vdots & & \frac{k_{i-1}(x_{i-1}-x_i)}{M_i} & 0 & & \\ & & & \ddots & & 0 \\ & & & & k_{N-1} & -1 \\ 0 & & \cdots & 0 & \frac{k_{N-1}(x_{N-1}-x_N)}{M_N} & \frac{x_N}{M_N} \end{bmatrix}$$

Note that u_N is not included in the vector of potential manipulated inputs ($\mathbf{u}_\mathrm{s}$) as it is typically set by the production rate.

The form in Eq. 2 is similar to the one introduced to capture generic recycle networks with large recycle of unconverted reactants s^{-1} (see Figure 2).[22] However, the structure of the corresponding matrices is different owing to the fact that no solute is recycled ($x_\mathrm{R} = 0$) in these *solvent* recycle networks, whereas significant amount of "solute" (i.e., unreacted species) is recycled ($x_\mathrm{R} = x_N$) in the generic recycle networks, as shown in Figure 2. This difference gives rise to unique analysis and control characteristics exhibited by these networks, as pointed out specifically in Remarks 1 and 5.

Model Reduction

In what follows, we apply the model reduction framework introduced in Kumar and Daoutidis[22] and identify unique features exhibited by this prototype network. Let us begin with the description of the dynamics in the fast time scale $\tau = t/\varepsilon$. In this "stretched" time scale, the dynamic equations in 2 become

$$\frac{d\mathbf{x}}{d\tau} = \varepsilon[\mathbf{f}(\mathbf{x}) + \mathbf{g}_\mathrm{s}(\mathbf{x})\mathbf{u}_\mathrm{s}] + \mathbf{g}_l(\mathbf{x})\mathbf{u}_l$$

Taking the limit $\varepsilon \to 0$, corresponding to an infinitely large recycle of solvent, the resulting equations describe the evolution of the network in the fast time scale

$$\frac{d\mathbf{x}}{d\tau} = \mathbf{g}_l(\mathbf{x})\mathbf{u}_l \tag{3}$$

It can be noted that all the process variables evolve in this fast time scale. However, only the scaled variables corresponding to the large internal flows affect the fast dynamics. This fast dynamics converges to a quasi-steady state, captured by the constraint equations

$$0 = \mathbf{g}_l(\mathbf{x})\mathbf{u}_l \tag{4}$$

It can be verified that these constraints are not linearly independent, resulting in an equilibrium manifold rather than an equilibrium point. Specifically, the last two constraints in Eq. 4 can be cast as a linear combination of the remaining $2(N-1)$ constraints, giving rise to a two-dimensional manifold where the slow dynamics evolves. Thus the constraints in Eq. 4 can be rewritten as

$$0 = \mathbf{B}(\mathbf{x})\tilde{\mathbf{g}}_l(\mathbf{x})\mathbf{u}_l \tag{5}$$

with

$$\tilde{\mathbf{g}}_l(\mathbf{x})\mathbf{u}_l = \begin{bmatrix} u_\mathrm{R} - k_1 u_1 \\ -u_\mathrm{R} x_1 \\ k_1 u_1 - k_2 u_2 \\ k_1 u_1 (x_1 - x_2) \\ \vdots \\ k_{N-2} u_{N-2} - k_{N-1} u_{N-1} \\ k_{N-2} u_{N-2} (x_{N-2} - x_{N-1}) \end{bmatrix}$$

being the linearly independent constraints, and

$$\mathbf{B}(\mathbf{x}) = \begin{bmatrix} 1 & 0 & \cdots & & 0 \\ 0 & \frac{1}{M_1} & & & \vdots \\ \vdots & & \ddots & & \\ & & & 1 & 0 \\ 0 & & & & \frac{1}{M_{N-1}} \\ -1 & 0 & -1 \quad 0 \quad \cdots & -1 & 0 \\ -\frac{(x_1-x_N)}{M_N} & -\frac{1}{M_N} & -\frac{(x_2-x_N)}{M_N} \quad -\frac{1}{M_N} \quad \cdots & -\frac{(x_{N-1}-x_N)}{M_N} & -\frac{1}{M_N} \end{bmatrix}$$

Considering the same limit $\varepsilon \to 0$ in the original time scale, Eq. 2 becomes

$$\begin{aligned} \frac{d\mathbf{x}}{dt} &= \mathbf{f}(\mathbf{x}) + \mathbf{g}_\mathrm{s}(\mathbf{x})\mathbf{u}_\mathrm{s} + \mathbf{B}(\mathbf{x}) \lim_{\varepsilon \to 0} \frac{\tilde{\mathbf{g}}_l(\mathbf{x})\mathbf{u}_l}{\varepsilon} \\ 0 &= \tilde{\mathbf{g}}_l(\mathbf{x})\mathbf{u}_l \end{aligned}$$

The limit terms correspond to the difference between the infinitely large internal flows which becomes indeterminate in this slow time scale. These indeterminate, yet finite terms are represented by a vector of so-called algebraic variables $\mathbf{z}$. The resulting description of the slow dynamics in the form of a set of differential algebraic equations (DAE) is

$$\begin{aligned} \frac{d\mathbf{x}}{dt} &= \mathbf{f}(\mathbf{x}) + \mathbf{g}_\mathrm{s}(\mathbf{x})\mathbf{u}_\mathrm{s} + \mathbf{B}(\mathbf{x})\mathbf{z} \\ 0 &= \tilde{\mathbf{g}}_l(\mathbf{x})\mathbf{u}_l \end{aligned} \tag{6}$$

The index of the DAE system in Eq. 6 is greater than 1. To get an equivalent ordinary differential equation (ODE) representation of the slow dynamics, the constraints need to be differentiated successively to reduce the index, ultimately

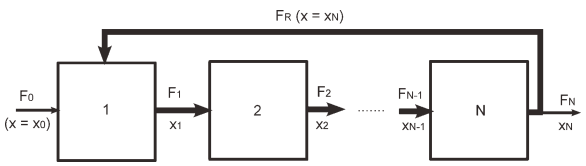

Figure 2. Generic network with large recycle of unreacted reactants $\mathbf{s}^{-1}$.[22]

obtaining functional forms of $\mathbf{z}$ (DAE with index 1) which can be substituted back in Eq. 6. Typically, one differentiation suffices which implies that no additional constraints are present and the slow dynamics is of dimension two. Before proceeding with this reduction, the internal material flows need to be either specified by a control law or assigned a constant value.

Alternatively, the slow dynamics of the network can also be expressed in terms of "true" slow variables which evolve solely in this time scale. One such variable is the total holdup of the network (M_{total}). Equation 7 represents the dynamic equation governing the evolution of the total network holdup

$$\frac{dM_{\text{total}}}{dt} = F_{0,\text{s}}\left[u_0 + u_{\text{A}} - k_N u_N + \sum_{i=2}^{N} k_{d,i} u_{d,i}\right] \tag{7}$$

which does not contain any large term, thus causing M_{total} to evolve over a longer time horizon. Similarly, the total holdup of the solvent (M_{solvent}) in the network, as evident from Eq. 8, also evolves entirely in the slow time scale

$$\frac{dM_{\text{solvent}}}{dt} = F_{0,\text{s}}\left[u_0 - k_N u_N(1 - x_N) + \sum_{i=2}^{N} k_{d,i} u_{d,i}(1 - x_{d,i})\right] \tag{8}$$

Remark 1 *The quasi-steady state constraints in Eq. 4 can be partitioned in two distinct blocks, one block* ($\mathbf{g}_l^{\text{holdup}}(\mathbf{x})u_l = 0$) *corresponding to the ones coming from the total material balance equations and the other* ($\mathbf{g}_l^{\text{species}}(\mathbf{x})\mathbf{u}_l = 0$) *from the species balance equations. The last constraint in each block can be cast as a linear combination of the first* $(N - 1)$ *constraints. The first* $(N - 1)$ *constraints in* $\mathbf{g}_l^{\text{species}}(\mathbf{x})\mathbf{u}_l = 0$ *can be solved, leading to*

$$x_i = 0 \qquad i = 1, 2, \ldots, (N-1) \tag{9}$$

and the last constraint leads to

$$-(k_{N-1}u_{N-1} - u_{\text{R}})x_N = 0$$

which makes x_N *indeterminate.*

The solutions in Eq. 9 *are the direct result of the infinitely large solvent recycle, leading to a strongly dilute environment in the first* $(N - 1)$ *process units. This offers great simplification in a model-based purity* (x_N) *controller, reducing the need for concentration sensors/estimators to just one.*

In the case of the generic network in Figure 2, *the quasi-steady state constraints arising from the fast dynamics can also be partitioned in two blocks:* $\mathbf{g}_l^{\text{holdup}}(\mathbf{x})\mathbf{u}_l = 0$ *and* $\overline{\mathbf{g}}_l^{\text{species}}(\mathbf{x})\mathbf{u}_l = 0$. *However, the corresponding species balance constraints* $\overline{\mathbf{g}}_l^{\text{species}}(\mathbf{x})\mathbf{u}_l = 0$ *cannot be solved explicitly, leading to a one-dimensional manifold characterized by*

$$x_1 = x_2 = \cdots = x_N$$

for each species in the recycle stream.

Remark 2 *The analysis presented so far is for single solute systems but can easily be extended for the case of multisolute systems. In the case of a system with c solutes,* $(c + 1)(N - 1)$ *constraints in Eq. 4 will be linearly independent, resulting in a* $(c + 1)$*-dimensional slow dynamics.*

Remark 3 *The prototype network assumes that the recycle flow does not contain any solute* ($x_{\text{R}} = 0$). *This assumption can be relaxed for relatively pure solvent recycles such that* x_{R} *is* $\mathcal{O}(\varepsilon)$. *The key results derived for the prototype network hold for such systems as well.*

Remark 4 *The analysis presented in this article addresses only the time scale multiplicity in the material balance equations, since the defining characteristics of the class of networks considered herein are the result of dominant material flows. As material flows also act as energy carriers, the large solvent recycle also induces stiffness in the corresponding energy balance equations, showing potential for time scale multiplicity in the energy dynamics as well. To this end, the existing results*[23–25] *addressing energetic effects of integrated networks can be used in conjunction with the results presented in this paper.*

Hierarchical Control

The two time-scale dynamics allows for the design of a hierarchical control scheme, wherein each tier of the controller addresses control objectives in each time scale. Specifically:

- **Fast control:** The material holdups of each unit should be regulated in this time scale. The large internal flows can be used as manipulated inputs through a control law of the form

$$\mathbf{u}_l = \mathbf{k}(\mathbf{x}) \tag{10}$$

- **Slow control:** The primary control objective of such networks is the control of the exit solute purity x_N, which should be controlled in this time scale. The large internal flows used to regulate individual unit holdups do not affect the total holdup of the network. The total holdup (especially the total solvent holdup) is affected only by the small external flows $\mathbf{u}_{\text{s}}$ (and the flows $u_{d,i}$) and thus also needs to be controlled in this time scale.

Having specified the internal flows through Eq. 10, the constraints in Eq. 6 become

$$0 = \tilde{\mathbf{g}}_l(\mathbf{x})\mathbf{k}(\mathbf{x}) = \phi(\mathbf{x}) \tag{11}$$

Differentiating this constraint (Eq. 11) once and substituting for $d\mathbf{x}/dt$ from Eq. 6 yields

$$\mathbf{z} = -\left[\mathcal{L}_{\mathbf{B}(\mathbf{x})}\phi(\mathbf{x})\right]^{-1}\left\{\mathcal{L}_{\mathbf{f}(\mathbf{x})}\phi(\mathbf{x}) + \mathcal{L}_{\mathbf{g}_{\text{s}}(\mathbf{x})}\phi(\mathbf{x})\ \mathbf{u}_{\text{s}}\right\} \tag{12}$$

where $\mathcal{L}$ denotes a Lie derivative. It can be verified that the matrix $\mathcal{L}_{\mathbf{B}(\mathbf{x})}\phi(\mathbf{x})$ is nonsingular irrespective of the choice of the control law (Eq. 10). Substituting for $\mathbf{z}$ in Eq. 6 gives the dynamic model capturing the evolution of the system in the slow time scale

$$\begin{aligned}\frac{d\mathbf{x}}{dt} = &\left[\mathbf{f}(\mathbf{x}) - \mathbf{B}(\mathbf{x})\left\{\mathcal{L}_{\mathbf{B}(\mathbf{x})}\phi(\mathbf{x})\right\}^{-1}\mathcal{L}_{\mathbf{f}(\mathbf{x})}\phi(\mathbf{x})\right] \\ &+ \left[\mathbf{g}_{\text{s}}(\mathbf{x}) - \mathbf{B}(\mathbf{x})\left\{\mathcal{L}_{\mathbf{B}(\mathbf{x})}\phi(\mathbf{x})\right\}^{-1}\mathcal{L}_{\mathbf{g}_{\text{s}}(\mathbf{x})}\phi(\mathbf{x})\right]\mathbf{u}_{\text{s}}\end{aligned} \tag{13}$$

subject to the constraint in Eq. 11. This slow model can be used to design a model-based controller to achieve the control objectives in this time scale.

Control of Prototype Network

Let us consider an illustrative example system with three units. The nominal values of the process parameters are tabulated in Table 1. The individual unit holdups are

Table 1. Nominal Values of Process Parameters for the Prototype Network with three Units

F_1	1000 mol s^{-1}	x_1	0.003
F_2	1007 mol s^{-1}	x_2	0.0037
F_3	25 mol s^{-1}	x_3	0.148
F_0	15 mol s^{-1}	M_1	1000 mol
F_A	3 mol s^{-1}	M_2	1000 mol
F_R	982 mol s^{-1}	M_3	1000 mol
d_2	7 mol s^{-1}	$x_{d,2}$	0.1
d_3	0 mol s^{-1}	$\mathcal{R}_i(x_i)$	0

regulated in the fast time scale using the following control law (Eq. 14):

$$\begin{bmatrix} u_1 \\ u_2 \\ u_R \end{bmatrix} = \mathbf{k}(\mathbf{x}) = \begin{bmatrix} 1 - K_{C,1}(M_{1,\text{set}} - M_1) \\ 1 - K_{C,2}(M_{2,\text{set}} - M_2) \\ 1 - K_{C,3}(M_{3,\text{set}} - M_3) \end{bmatrix} \tag{14}$$

This control law was used to derive the slow model (Eq. 13). Figure 3 shows the open-loop response of the product purity x_3 for a 10% disturbance in d_2 and -1% disturbance in $x_{d,2}$. Except for the initial transient, the full model (solid line) and the slow model (dotted line) match very closely. This slow model was then used to derive a nonlinear output feedback controller[27] to control the product purity ($y_1 = x_3$) and the total material holdup ($y_2 = M_1 + M_2 + M_3$). Relative degrees for both the outputs are 1 and hence we requested first order decoupled responses of the form shown in Eq. 15:

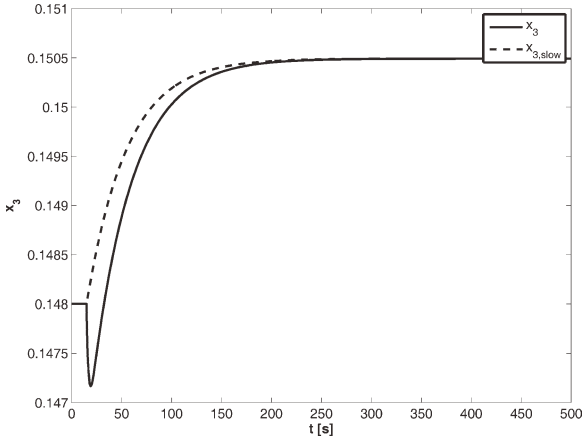

Figure 3. Open loop response of the product purity in the presence of a disturbance in $u_{d,2}$ and $x_{d,2}$.

$$\begin{aligned} \beta_1 \frac{dy_1}{dt} + y_1 &= y_{1,\text{set}} \\ \beta_2 \frac{dy_2}{dt} + y_2 &= y_{2,\text{set}} \end{aligned} \tag{15}$$

with $\beta_1 = \beta_2 = \beta = 100$ s. We also compared the performance of this reduced order controller with a controller derived on the basis of the full model from Eq. 2. In this case, the relative

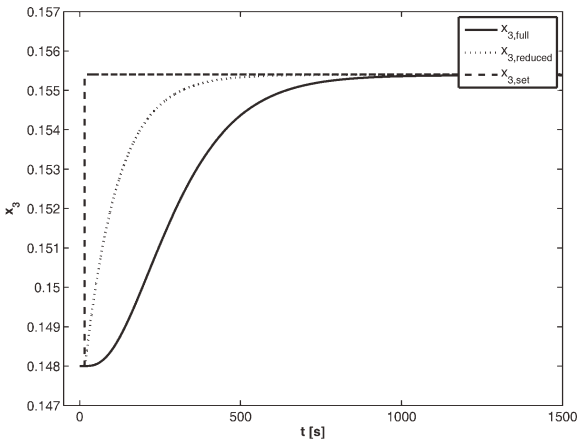

(a) x_3

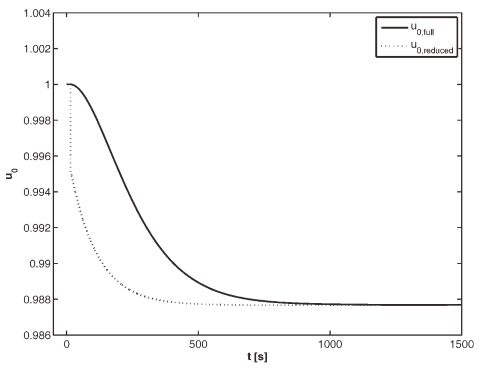

(b) u_0

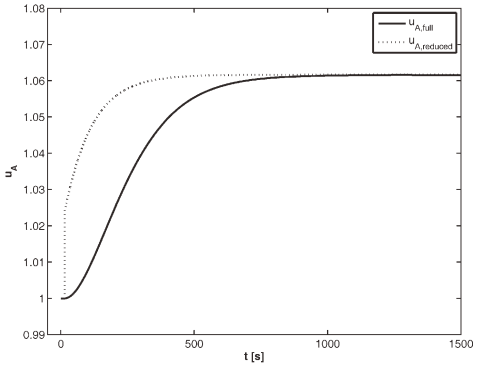

(c) u_A

Figure 4. Response of the prototype system for a set point change.

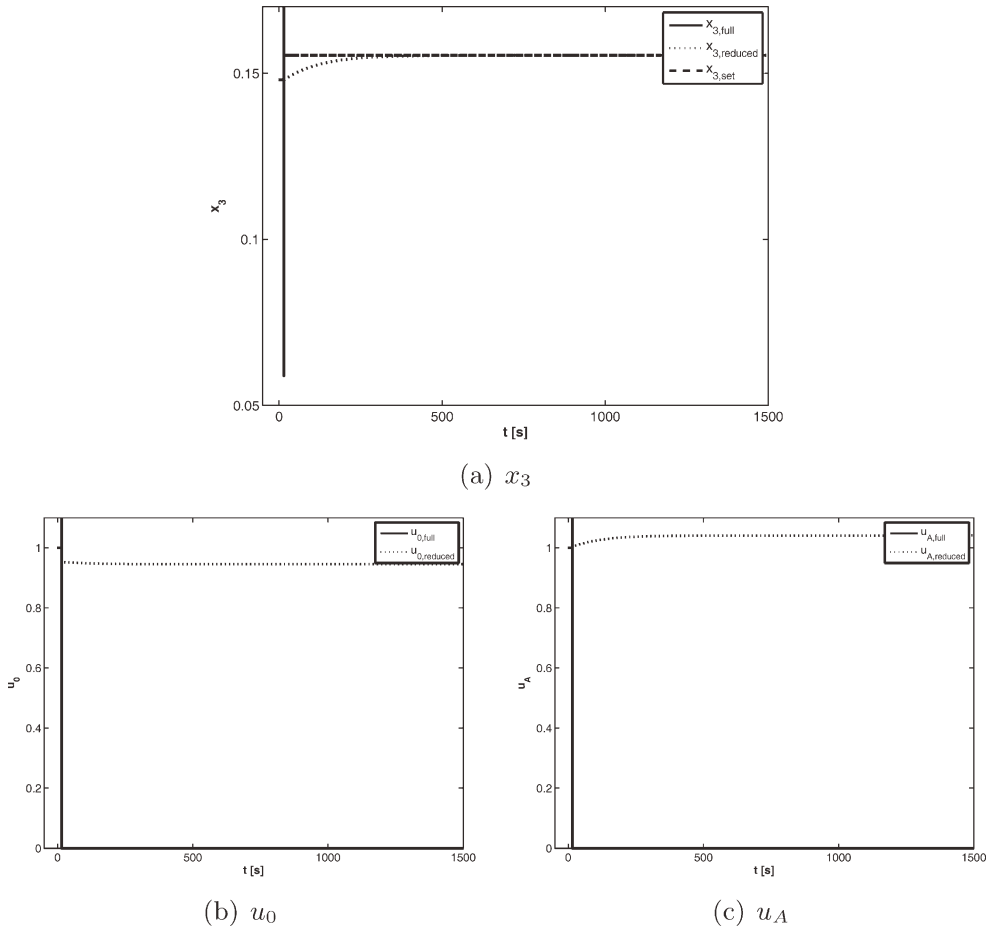

(a) x_3

(b) u_0

(c) u_A

Figure 5. Response of the prototype system for a set point change in the presence of disturbances.

degree for y_1 and y_2 is 3 and 1, respectively. So we requested decoupled responses of the form

$$\beta_{13}\frac{d^3y_1}{dt^3}+\beta_{12}\frac{d^2y_1}{dt^2}+\beta_{11}\frac{dy_1}{dt}+y_1=y_{1,\text{set}}$$
$$\beta_{21}\frac{dy_2}{dt}+y_2=y_{2,\text{set}} \tag{16}$$

with $\beta_{13}=\beta^3$, $\beta_{12}=3\,\beta^2$, $\beta_{11}=3\,\beta$, and $\beta_{21}=\beta=100$ s.

In the first simulation run, we considered a 5% increase in the purity set point and the corresponding responses are shown in Figure 4. Both the full model-based and reduced model-based controller achieved smooth steady state transition. For the same time constant, the reduced order controller is faster than the full order controller as it requests a lower order (first compared to third) response. The initial aggressive action in the manipulated variables, in the case of the reduced order controller, is due to the mismatch between the fast dynamics of the actual process model and the slow model used for controller derivation.

In the next simulation run, we considered the same set point change, but in the presence of a 10% disturbance in d_2 and -1% disturbance in $x_{d,2}$. Figure 5 shows the corresponding responses. The full model-based controller is very sensitive to disturbances and fails to achieve the requested set point transition. This was expected as the underlying model used for controller derivation was stiff.[26,28] However, the reduced order controller yields the requested purity set point and is quite robust to disturbances (see Figure 6).

Remark 5 *The relative degree of x_N on the basis of the reduced order slow model will always be 1, irrespective of the control law (Eq. 10) and the number of process units N. The relative degree of x_N on the basis of the full model, however, depends on the control law. Specifically, if the individual unit holdups are regulated through the exit flows as in Eq. 14, the relative degree for x_N is N. On the other hand, if the individual unit holdups are regulated via inlet flows, the relative degree for x_N is* 1*, with a structurally singular characteristic matrix, ultimately resulting in a higher order nonlinear controller.*[29] *The above illustrate further the advantages of the proposed model reduction and control framework.*

For the generic network in Figure 2*, the relative degree of x_N on the basis of the corresponding full model is N, irrespective of the corresponding fast control law (Eq. 10).*

Control of a Biphasic System for HMF Production

Let us now consider an application of the proposed framework to a newly proposed and more complex system, namely the one of HMF production from fructose. HMF is a furanic compound considered to be a key intermediate in the production of biomass-derived fuels and chemicals. In particular, HMF can be used to synthesize building blocks for the production of polymer (e.g., polyethylene terephthalate,

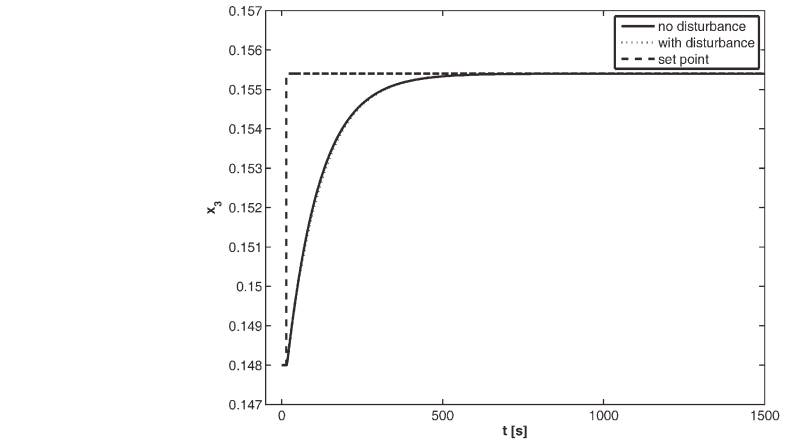

(a) x_3

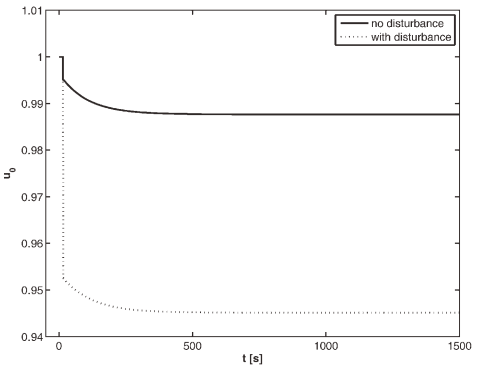

(b) u_0

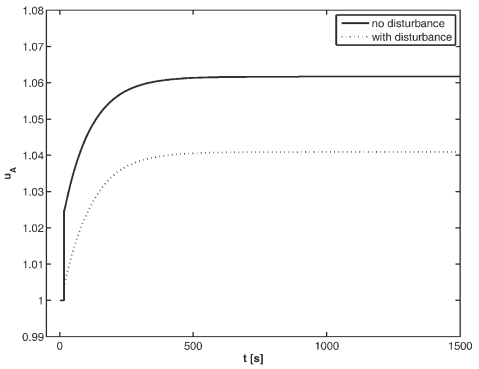

(c) u_A

Figure 6. Response of the prototype system for a set point change in the presence of disturbances.

polybutylene terephthalate) analogs, which are currently derived from oil.

The acid-catalyzed dehydration of fructose in aqueous media for HMF production is highly non-selective leading to several soluble and insoluble products apart from HMF. In addition, HMF further reacts in water producing mainly levulinic and formic acids, and fructose–fructose and fructose–HMF oligomers. Figure 7 shows a simplified kinetic model for this system.[30] This model accounts for the losses of fructose (A) due to the formation of products other than HMF (B) lumping them under a single term (BPA), neglects the existence of intermediate products between fructose and HMF, considers levulinic (C) and formic acids (D) as the main HMF rehydration products and lumps the rest of the byproducts into a single term (BPB).

In previous work,[31] a continuous process for the production of HMF using a biphasic system with an organic phase that selectively extracts the HMF produced (as proposed in Roman-Leshkov et al.[12]) was designed and optimized. As shown in Figure 8, the process consists of a biphasic reactor coupled with an extractor and an evaporator. Here, a solution containing fructose and catalyst are fed to a continuously stirred biphasic tank reactor. The reaction takes place in the aqueous phase while the organic phase composed of 7:3 methyl *iso*-butylketone:2-butanol selectively extracts the HMF produced, thus minimizing its decomposition. The aqueous stream exiting the reactor is sent to a liquid–liquid extractor to recover the fraction of HMF that remains in it,

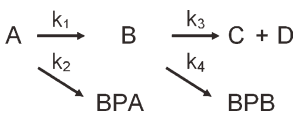

Figure 7. Reactions taking place in HMF production.

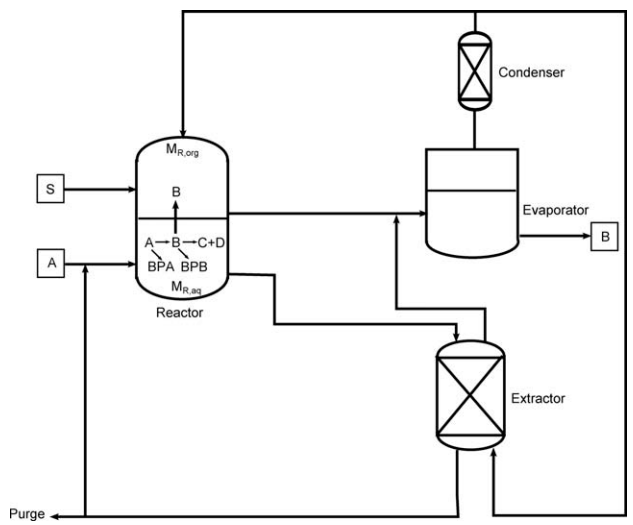

Figure 8. Process for the production of HMF (A: fructose, BPA: byproducts from fructose, B: HMF, C: levulinic acid, D: formic acid, BPB: other decomposition products from HMF, S: solvent).

and is then recycled back to the reactor. A purge stream is required to prevent the accumulation of byproducts in the reactor aqueous phase. The streams exiting the organic phase of the reactor and the extractor are sent to the evaporator, from where purified HMF is obtained as the product. The evaporated solvent is recycled back to the extractor and the reactor. A small amount of fresh solvent is also added to the organic phase of the reactor to maintain the solvent inventory in the system.

The system is required to produce HMF with specified purity and flow rate. The values of the process parameters used in this example correspond to the optimal steady state in section 4.4 of Torres et al.[31] and are tabulated in Table 2. We can note that the optimal steady state is characterized by the presence of:

- a large solvent recycle flow (v_8 and v_9) compared to fresh solvent feed flow (v_{S0});
- a negligible amount of HMF in the solvent recycle stream, and
- dilute streams in all the units except the evaporator.

Figure 9 schematically represents the various flows in this system, with the flows of different orders of magnitude distinguished via lines of different thickness. We can notice the presence of the prototype network, albeit in a modified form. Specifically, there are two pure solute streams N_B and N_{EB}, and two large solvent recycles, one via the reactor (v_8) and the other via the liquid–liquid extractor (v_9).

The dynamic material balance equations for this system are given as:

Reactor:

$$\frac{dM_{R,aq}}{dt} = v_0 + v_r - v_1 + 3\aleph_1 x_{A,1} M_{R,aq} - \aleph_3 x_{B,1} M_{R,aq} - N_B$$

$$\frac{dx_{A,1}}{dt} = \frac{1}{M_{R,aq}}\left[v_0(x_{A,0} - x_{A,1}) + v_r(x_{A,2} - x_{A,1}) - (1 + 3x_{A,1})\aleph_1 x_{A,1} M_{R,aq} - \aleph_2 x_{A,1} M_{R,aq} + x_{A,1}\aleph_3 x_{B,1} M_{R,aq} + x_{A,1} N_B\right]$$

$$\frac{dx_{B,1}}{dt} = \frac{1}{M_{R,aq}}\left[-x_{B,1} v_0 + v_r(x_{B,2} - x_{B,1}) + (1 - 3x_{B,1})\aleph_1 x_{A,1} M_{R,aq} - (1 - x_{B,1})\aleph_3 x_{B,1} M_{R,aq} - \aleph_4 x_{B,1} M_{R,aq} - (1 - x_{B,1}) N_B\right]$$

$$\frac{dx_{BPA,1}}{dt} = \frac{1}{M_{R,aq}}\left[-x_{BPA,1} v_0 + v_r(x_{BPA,2} - x_{BPA,1}) - 3x_{BPA,1}\aleph_1 x_{A,1} M_{R,aq} + \aleph_2 x_{A,1} M_{R,aq} + x_{BPA,1}\aleph_3 x_{B,1} M_{R,aq} + x_{BPA,1} N_B\right]$$

$$\frac{dx_{BPB,1}}{dt} = \frac{1}{M_{R,aq}}\left[-x_{BPB,1} v_0 + v_r(x_{BPB,2} - x_{BPB,1}) - 3x_{BPB,1}\aleph_1 x_{A,1} M_{R,aq} + x_{BPB,1}\aleph_3 x_{B,1} M_{R,aq} + \aleph_4 x_{B,1} M_{R,aq} + x_{BPB,1} N_B\right]$$

$$\frac{dx_{W,1}}{dt} = \frac{1}{M_{R,aq}}\left[v_0(x_{W,0} - x_{W,1}) + v_r(x_{W,2} - x_{W,1}) + 3(1 - x_{W,1})\aleph_1 x_{A,1} M_{R,aq} - (2 - x_{W,1})\aleph_3 x_{B,1} M_{R,aq} + x_{W,1} N_B\right]$$

$$\frac{dM_{R,org}}{dt} = v_{S0} + v_8 - v_4 + N_B$$

$$\frac{dx_{B,4}}{dt} = \frac{1}{M_{R,org}}\left[(1 - x_{B,4})N_B - x_{B,4}(v_{S0} + v_8)\right]$$

Liquid–liquid extractor:

$$\frac{dM_{Ex,aq}}{dt} = v_1 - v_2 - N_{EB}$$

$$\frac{dx_{A,2}}{dt} = \frac{1}{M_{Ex,aq}}\left[v_1(x_{A,1} - x_{A,2}) + x_{A,2} N_{EB}\right]$$

$$\frac{dx_{B,2}}{dt} = \frac{1}{M_{Ex,aq}}\left[v_1(x_{B,1} - x_{B,2}) - (1 - x_{B,2})N_{EB}\right]$$

$$\frac{dx_{BPA,2}}{dt} = \frac{1}{M_{Ex,aq}}\left[v_1(x_{BPA,1} - x_{BPA,2}) + x_{BPA,2} N_{EB}\right]$$

$$\frac{dx_{BPB,2}}{dt} = \frac{1}{M_{Ex,aq}}\left[v_1(x_{BPB,1} - x_{BPB,2}) + x_{BPB,2} N_{EB}\right]$$

$$\frac{dx_{W,2}}{dt} = \frac{1}{M_{Ex,aq}}\left[v_1(x_{W,1} - x_{W,2}) + x_{W,2} N_{EB}\right]$$

$$\frac{dM_{Ex,org}}{dt} = v_9 + N_{EB} - v_3$$

$$\frac{dx_{B,3}}{dt} = \frac{1}{M_{Ex,org}}\left[-x_{B,3} v_9 + (1 - x_{B,3})N_{EB}\right]$$

Evaporator:

$$\frac{dM_{Ev}}{dt} = v_3 + v_4 - v_8 - v_9$$

$$\frac{dx_{B,6}}{dt} = \frac{1}{M_{Ev}}\left[v_3(x_{B,3} - x_{B,6}) + v_4(x_{B,4} - x_{B,6}) + x_{B,6}(v_8 + v_9)\right] \quad (17)$$

Assuming fast mass transfer rate, the flows N_B and N_{EB} can be given by (see Kumar and Daoutidis[32] for details of the derivation)

$$N_B = \frac{1}{1 - x_{B,4} + \alpha_R(1 - x_{B,1})} \times \left[\alpha_R\left\{-x_{B,1} v_0 + v_r(x_{B,2} - x_{B,1}) + (1 - 3x_{B,1})\aleph_1 x_{A,1} M_{R,aq} - (1 - x_{B,1})\aleph_3 x_{B,1} M_{R,aq} - \aleph_4 x_{B,1} M_{R,aq}\right\} + x_{B,4}(v_{S0} + v_8)\right]$$

$$N_{EB} = \frac{1}{1 - x_{B,3} - \alpha_{Ex}(1 - x_{B,2})} \times \left[x_{B,3} v_9 + \alpha_{Ex} v_1(x_{B,2} - x_{B,1})\right]$$

where $\alpha_R = \kappa \frac{\rho_{aq} M_{R,org}}{\rho_{org} M_{R,aq}}$ and $\alpha_{Ex} = \kappa \frac{\rho_{aq} M_{Ex,org}}{\rho_{org} M_{Ex,aq}}$.

Table 2. Nominal Values of Process Parameters for the Biphasic System for HMF Production

$x_{A,1}$	0.0036	v_{S0}	5.81×10^0 mol min^{-1}
$x_{B,1}$	0.0022	v_0	6.85×10^3 mol min^{-1}
$x_{BPA,1}$	0.0179	v_1	1.56×10^4 mol min^{-1}
$x_{BPB,1}$	0.0008	v_2	1.56×10^4 mol min^{-1}
$x_{W,1}$	0.9740	v_3	1.89×10^3 mol min^{-1}
$x_{A,2}$	0.0036	v_4	3.47×10^3 mol min^{-1}
$x_{B,2}$	0.0009	v_6	1.16×10^2 mol min^{-1}
$x_{BPA,2}$	0.0180	v_8	3.37×10^3 mol min^{-1}
$x_{BPB,2}$	0.0009	v_9	1.87×10^3 mol min^{-1}
$x_{W,2}$	0.9753	v_r	8.43×10^3 mol min^{-1}
$x_{B,3}$	0.0108	N_B	9.00×10^1 mol min^{-1}
$x_{B,4}$	0.0259	N_{EB}	2.04×10^1 mol min^{-1}
$x_{B,6}$	0.9500	$\aleph_1$	0.9218 min^{-1}
$M_{R,aq}$	3.87×10^4 mol	$\aleph_2$	0.9218 min^{-1}
$M_{R,org}$	8.62×10^3 mol	$\aleph_3$	0.0548 min^{-1}
$M_{Ex,aq}$	3.87×10^3 mol	$\aleph_4$	0.0698 min^{-1}
$M_{Ex,org}$	8.62×10^2 mol	$x_{A,0}$	0.0411
M_{Ev}	3.87×10^4 mol	$x_{W,0}$	0.9589

Defining $\mathcal{O}(1)$ steady state ratios and scaled flows as tabulated in Table 3, the above dynamic equations can be cast in the vector form (Eq. 2) with

$$\mathbf{x} = \begin{bmatrix} M_{\mathrm{R,aq}} & x_{\mathrm{A},1} & x_{\mathrm{B},1} & x_{\mathrm{BPA},1} & x_{\mathrm{BPB},1} & x_{\mathrm{W},1} & M_{\mathrm{R,org}} & x_{\mathrm{B},4} M_{\mathrm{Ex,aq}} \\ x_{\mathrm{A},2} & x_{\mathrm{B},2} & x_{\mathrm{BPA},2} & x_{\mathrm{BPB},2} & x_{\mathrm{W},2} & M_{\mathrm{Ex,org}} & x_{\mathrm{B},3} & M_{\mathrm{Ev}}\, x_{\mathrm{B},6} \end{bmatrix}^T$$

$$\mathbf{u}_{\mathrm{s}} = \begin{bmatrix} u_{\mathrm{S0}} & u_{\mathrm{NB}} & u_{\mathrm{NEB}} \end{bmatrix}^T$$

$$\mathbf{u}_l = \begin{bmatrix} u_0 & u_1 & u_2 & u_3 & u_4 & u_8 & u_9 & u_r \end{bmatrix}^T$$

$$\varepsilon = \frac{v_{S0,\mathrm{s}}}{v_{8,\mathrm{s}}}$$

$$\mathbf{f}(\mathbf{x}) = v_{S0,\mathrm{s}} \begin{bmatrix} 3k_{r,1}\left(\frac{x_{\mathrm{A},1}}{x_{\mathrm{A},1,\mathrm{s}}}\right)\left(\frac{M_{\mathrm{R,aq}}}{M_{\mathrm{R,aq,s}}}\right) - k_{r,3}\left(\frac{x_{\mathrm{B},1}}{x_{\mathrm{B},1,\mathrm{s}}}\right)\left(\frac{M_{\mathrm{R,aq}}}{M_{\mathrm{R,aq,s}}}\right) \\ -\frac{(1+3x_{\mathrm{A},1})k_{r,1}}{M_{\mathrm{R,aq}}}\left(\frac{x_{\mathrm{A},1}}{x_{\mathrm{A},1,\mathrm{s}}}\right)\left(\frac{M_{\mathrm{R,aq}}}{M_{\mathrm{R,aq,s}}}\right) - \frac{k_{r,2}}{M_{\mathrm{R,aq}}}\left(\frac{x_{\mathrm{A},1}}{x_{\mathrm{A},1,\mathrm{s}}}\right)\left(\frac{M_{\mathrm{R,aq}}}{M_{\mathrm{R,aq,s}}}\right) + \frac{x_{\mathrm{A},1}k_{r,3}}{M_{\mathrm{R,aq}}}\left(\frac{x_{\mathrm{B},1}}{x_{\mathrm{B},1,\mathrm{s}}}\right)\left(\frac{M_{\mathrm{R,aq}}}{M_{\mathrm{R,aq,s}}}\right) \\ \frac{(1-3x_{\mathrm{B},1})k_{r,1}}{M_{\mathrm{R,aq}}}\left(\frac{x_{\mathrm{A},1}}{x_{\mathrm{A},1,\mathrm{s}}}\right)\left(\frac{M_{\mathrm{R,aq}}}{M_{\mathrm{R,aq,s}}}\right) - \frac{(1-x_{\mathrm{B},1})k_{r,3}}{M_{\mathrm{R,aq}}}\left(\frac{x_{\mathrm{B},1}}{x_{\mathrm{B},1,\mathrm{s}}}\right)\left(\frac{M_{\mathrm{R,aq}}}{M_{\mathrm{R,aq,s}}}\right) - \frac{k_{r,4}}{M_{\mathrm{R,aq}}}\left(\frac{x_{\mathrm{B},1}}{x_{\mathrm{B},1,\mathrm{s}}}\right)\left(\frac{M_{\mathrm{R,aq}}}{M_{\mathrm{R,aq,s}}}\right) \\ -\frac{3x_{\mathrm{BPA},1}k_{r,1}}{M_{\mathrm{R,aq}}}\left(\frac{x_{\mathrm{A},1}}{x_{\mathrm{A},1,\mathrm{s}}}\right)\left(\frac{M_{\mathrm{R,aq}}}{M_{\mathrm{R,aq,s}}}\right) + \frac{k_{r,2}}{M_{\mathrm{R,aq}}}\left(\frac{x_{\mathrm{A},1}}{x_{\mathrm{A},1,\mathrm{s}}}\right)\left(\frac{M_{\mathrm{R,aq}}}{M_{\mathrm{R,aq,s}}}\right) + \frac{x_{\mathrm{BPA},1}k_{r,3}}{M_{\mathrm{R,aq}}}\left(\frac{x_{\mathrm{B},1}}{x_{\mathrm{B},1,\mathrm{s}}}\right)\left(\frac{M_{\mathrm{R,aq}}}{M_{\mathrm{R,aq,s}}}\right) \\ -\frac{3x_{\mathrm{BPB},1}k_{r,1}}{M_{\mathrm{R,aq}}}\left(\frac{x_{\mathrm{A},1}}{x_{\mathrm{A},1,\mathrm{s}}}\right)\left(\frac{M_{\mathrm{R,aq}}}{M_{\mathrm{R,aq,s}}}\right) + \frac{x_{\mathrm{BPB},1}k_{r,3}}{M_{\mathrm{R,aq}}}\left(\frac{x_{\mathrm{B},1}}{x_{\mathrm{B},1,\mathrm{s}}}\right)\left(\frac{M_{\mathrm{R,aq}}}{M_{\mathrm{R,aq,s}}}\right) + \frac{k_{r,4}}{M_{\mathrm{R,aq}}}\left(\frac{x_{\mathrm{B},1}}{x_{\mathrm{B},1,\mathrm{s}}}\right)\left(\frac{M_{\mathrm{R,aq}}}{M_{\mathrm{R,aq,s}}}\right) \\ \frac{3(1-x_{\mathrm{W},1})k_{r,1}}{M_{\mathrm{R,aq}}}\left(\frac{x_{\mathrm{A},1}}{x_{\mathrm{A},1,\mathrm{s}}}\right)\left(\frac{M_{\mathrm{R,aq}}}{M_{\mathrm{R,aq,s}}}\right) - \frac{(2-x_{\mathrm{W},1})k_{r,3}}{M_{\mathrm{R,aq}}}\left(\frac{x_{\mathrm{B},1}}{x_{\mathrm{B},1,\mathrm{s}}}\right)\left(\frac{M_{\mathrm{R,aq}}}{M_{\mathrm{R,aq,s}}}\right) \\ 0 \\ 0 \\ 0 \\ 0 \\ 0 \\ 0 \\ 0 \\ 0 \\ 0 \\ 0 \\ -k_{v,6}u_{v,6} \\ 0 \end{bmatrix}$$

$$\mathbf{g}_l(\mathbf{x}) = v_{S0,\mathrm{s}} \begin{bmatrix} k_{v,0} & -k_{v,1} & & & & & & k_{v,r} \\ \frac{k_{v,0}(x_{\mathrm{A},0}-x_{\mathrm{A},1})}{M_{\mathrm{R,aq}}} & & & & & & & \frac{k_{v,r}(x_{\mathrm{A},2}-x_{\mathrm{A},1})}{M_{\mathrm{R,aq}}} \\ -\frac{k_{v,0}x_{\mathrm{B},1}}{M_{\mathrm{R,aq}}} & & & & & & & \frac{k_{v,r}(x_{\mathrm{B},2}-x_{\mathrm{B},1})}{M_{\mathrm{R,aq}}} \\ -\frac{k_{v,0}x_{\mathrm{BPA},1}}{M_{\mathrm{R,aq}}} & & & & & & & \frac{k_{v,r}(x_{\mathrm{BPA},2}-x_{\mathrm{BPA},1})}{M_{\mathrm{R,aq}}} \\ -\frac{k_{v,0}x_{\mathrm{BPB},1}}{M_{\mathrm{R,aq}}} & & & & & & & \frac{k_{v,r}(x_{\mathrm{BPB},2}-x_{\mathrm{BPB},1})}{M_{\mathrm{R,aq}}} \\ \frac{k_{v,0}(x_{\mathrm{W},0}-x_{\mathrm{W},1})}{M_{\mathrm{R,aq}}} & & & & & & & \frac{k_{v,r}(x_{\mathrm{W},2}-x_{\mathrm{W},1})}{M_{\mathrm{R,aq}}} \\ & & & & -k_{v,4} & \frac{1}{M_{\mathrm{R,org}}} & & \\ & & & & & -\frac{x_{\mathrm{B},4}}{M_{\mathrm{R,org}}} & & \\ & k_{v,1} & -k_{v,2} & & & & & \\ & \frac{k_{v,1}(x_{\mathrm{A},1}-x_{\mathrm{A},2})}{M_{\mathrm{Ex,aq}}} & & & & & & \\ & \frac{k_{v,1}(x_{\mathrm{B},1}-x_{\mathrm{B},2})}{M_{\mathrm{Ex,aq}}} & & & & & & \\ & \frac{k_{v,1}(x_{\mathrm{BPA},1}-x_{\mathrm{BPA},2})}{M_{\mathrm{Ex,aq}}} & & & & & & \\ & \frac{k_{v,1}(x_{\mathrm{BPB},1}-x_{\mathrm{BPB},2})}{M_{\mathrm{Ex,aq}}} & & & & & & \\ & \frac{k_{v,1}(x_{\mathrm{W},1}-x_{\mathrm{W},2})}{M_{\mathrm{Ex,aq}}} & & & & & & \\ & & & -k_{v,3} & & k_{v,9} & & \\ & & & & & -\frac{k_{v,9}x_{\mathrm{B},3}}{M_{\mathrm{Ex,org}}} & & \\ & & & k_{v,3} & k_{v,4} & -k_{v,8} & -k_{v,9} & \\ & & & \frac{k_{v,3}(x_{\mathrm{B},3}-x_{\mathrm{B},6})}{M_{\mathrm{Ev}}} & \frac{k_{v,4}(x_{\mathrm{B},4}-x_{\mathrm{B},6})}{M_{\mathrm{Ev}}} & \frac{k_{v,8}x_{\mathrm{B},6}}{M_{\mathrm{Ev}}} & \frac{k_{v,9}x_{\mathrm{B},6}}{M_{\mathrm{Ev}}} & \end{bmatrix}$$

$$\mathbf{g}_s(\mathbf{x}) = v_{S0,s}\begin{bmatrix} 0 & -k_{NB} & 0 \\ 0 & \frac{k_{NB}x_{A,1}}{M_{R,aq}} & 0 \\ 0 & -\frac{k_{NB}(1-x_{B,1})}{M_{R,aq}} & 0 \\ 0 & \frac{k_{NB}x_{BPA,1}}{M_{R,aq}} & 0 \\ 0 & \frac{k_{NB}x_{BPB,1}}{M_{R,aq}} & 0 \\ 0 & \frac{k_{NB}x_{W,1}}{M_{R,aq}} & 0 \\ 1 & k_{NB} & 0 \\ -\frac{x_{B,4}}{M_{R,org}} & \frac{k_{NB}(1-x_{B,4})}{M_{R,org}} & 0 \\ 0 & 0 & -k_{NEB} \\ 0 & 0 & \frac{k_{NEB}x_{A,2}}{M_{Ex,aq}} \\ 0 & 0 & -\frac{k_{NEB}(1-x_{B,2})}{M_{Ex,aq}} \\ 0 & 0 & \frac{k_{NEB}x_{BPA,2}}{M_{Ex,aq}} \\ 0 & 0 & \frac{k_{NEB}x_{BPB,2}}{M_{Ex,aq}} \\ 0 & 0 & \frac{k_{NEB}x_{W,2}}{M_{Ex,aq}} \\ 0 & 0 & k_{NEB} \\ 0 & 0 & \frac{k_{NEB}(1-x_{B,3})}{M_{Ex,org}} \\ 0 & 0 & 0 \\ 0 & 0 & 0 \end{bmatrix}$$

Following the model reduction approach as presented earlier, the description of the fast dynamics of this system similar to Eq. 3 can be obtained. The resulting quasi-steady state constraints are linearly dependent; however, in this case, only the constraints corresponding to the large organic solvent recycle are linearly dependent whereas the constraints corresponding to water recycle are linearly independent (owing to the large inlet and outlet flows). The independent constraints can be solved to get explicit expressions for the state variables corresponding to the water recycle loop. The analysis for the organic solvent recycle loop is performed along similar lines as the prototype network.

In the fast time scale, the holdups of all the process units are regulated using a control law of the form:

$$\begin{bmatrix} u_{v,1} \\ u_{v,2} \\ u_{v,3} \\ u_{v,4} \\ u_{v,8} \end{bmatrix} = \mathbf{k}(\mathbf{x}) = \begin{bmatrix} 1 - K_{C,1}(M_{R,aq,set} - M_{R,aq}) \\ 1 - K_{C,2}(M_{Ex,aq,set} - M_{Ex,aq}) \\ 1 - K_{C,3}(M_{Ex,org,set} - M_{Ex,org}) \\ 1 - K_{C,4}(M_{R,org,set} - M_{R,org}) \\ 1 - K_{C,8}(M_{Ev,set} - M_{Ev}) \end{bmatrix} \quad (18)$$

Using the control of the form of Eq. 13, an ODE representation of the slow dynamics of the form of Eq. 13 was obtained and used for the derivation of the model-based controller. In this slow time scale, the control objectives include the purity of the product ($y_1 = x_{B,6}$) and the total holdup of the solvent recycle network ($y_2 = M_{R,org} + M_{Ex,org} + M_{Ev}$). The small flows $u_{v,S0}$, u_{NB}, and u_{NEB} are the potential manipulated inputs. Note that the small flow $u_{v,6}$ is not considered as a manipulated input as it is set by the production rate. For this study, we chose u_{S0} and u_{NB} to be the manipulated inputs for the slow controller and treated u_{NEB} as an unmeasured disturbance. However, the mass transfer rates across the reactor (u_{NB}) (or the extractor (u_{NEB})) cannot be manipulated directly. A fast proportional (P) controller (Eq. 19) was therefore implemented

$$u_{v,0} = 1 - K_{C,0}(u_{NB,set} - u_{NB}) \quad (19)$$

resulting in a cascade configuration. The resulting overall control system is as shown in Figure 10. For the slow control,

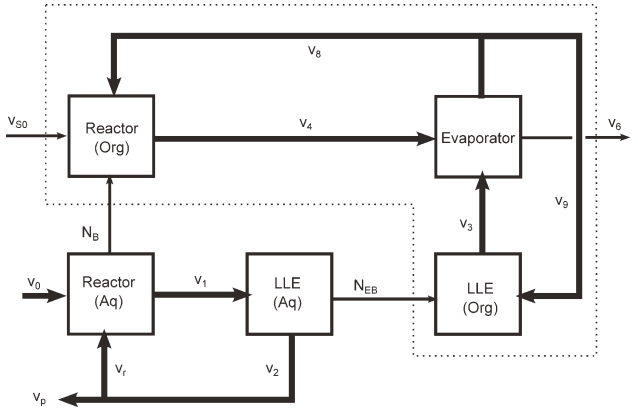

Figure 9. Schematic representation of flows in the biphasic system for HMF production.

we designed a nonlinear input/output linearizing controller. The relative degree for both the outputs (y_1 and y_2) is 1 and we requested first-order responses of the form 20 with $\beta = 200$ min. To get offset-free response, the model-based controller was augmented by an external proportional integral (PI) controller for the purity loop

$$\beta\frac{dy_1}{dt} + y_1 = y_{1,set} + \left((y_{1,set} - y_1) + \frac{1}{\beta}\int_0^t (y_{1,set} - y_1)d\tau\right)$$
$$\beta\frac{dy_2}{dt} + y_2 = y_{2,set} \quad (20)$$

Several simulation scenarios were considered to test the performance of the proposed control strategy. In the first run, the purity of the product was changed from 95% to 97.5% and the corresponding closed-loop responses are shown in Figure 11. The proposed control strategy enables smooth transition between the steady states. The initial agressive

Table 3. $\mathcal{O}(1)$ Steady State Ratios and Scaled Flows

Steady State Ratios	Scaled Flows
$k_{v,0} = \frac{v_{0,s}}{v_{8,s}}$	$u_{v,0} = \frac{v_0}{v_{0,s}}$
$k_{v,1} = \frac{v_{1,s}}{v_{8,s}}$	$u_{v,1} = \frac{v_1}{v_{1,s}}$
$k_{v,2} = \frac{v_{2,s}}{v_{8,s}}$	$u_{v,2} = \frac{v_2}{v_{2,s}}$
$k_{v,3} = \frac{v_{3,s}}{v_{8,s}}$	$u_{v,3} = \frac{v_3}{v_{3,s}}$
$k_{v,4} = \frac{v_{4,s}}{v_{8,s}}$	$u_{v,4} = \frac{v_4}{v_{4,s}}$
$k_{v,9} = \frac{v_{9,s}}{v_{8,s}}$	$u_{v,9} = \frac{v_9}{v_{9,s}}$
$k_{v,r} = \frac{v_{r,s}}{v_{8,s}}$	$u_{v,r} = \frac{v_r}{v_{r,s}}$
$k_{v,p} = \frac{v_{p,s}}{v_{8,s}}$	$u_{v,p} = \frac{v_p}{v_{p,s}}$
$k_{v,6} = \frac{v_{6,s}}{v_{S0,s}}$	$u_{v,6} = \frac{v_6}{v_{6,s}}$
$k_{NB} = \frac{N_{B,s}}{v_{S0,s}}$	$u_{NB} = \frac{N_B}{N_{B,s}}$
$k_{NEB} = \frac{N_{EB,s}}{v_{S0,s}}$	$u_{NEB} = \frac{N_{EB}}{N_{EB,s}}$
$k_{r,1} = \frac{\aleph_1 x_{A,1} M_{R,aq}}{v_{S0,s}}$	$u_{v,S0} = \frac{v_{S0}}{v_{S0,s}}$
$k_{r,2} = \frac{\aleph_2 x_{A,1} M_{R,aq}}{v_{S0,s}}$	$u_{v,8} = \frac{v_8}{v_{8,s}}$
$k_{r,3} = \frac{\aleph_3 x_{B,1} M_{R,aq}}{v_{S0,s}}$	
$k_{r,4} = \frac{\aleph_4 x_{B,1} M_{R,aq}}{v_{S0,s}}$	

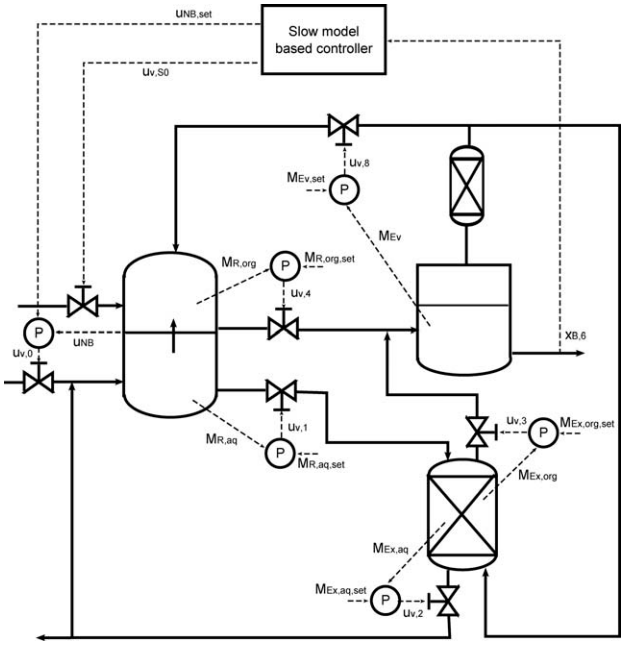

Figure 10. Control system for the biphasic system for HMF production.

action is again due to the mismatch between the dynamic and the controller model. In the next run, a 5% error in modeling the kinetic rate constant k_1 was considered, along with the increase in the product purity. The corresponding plots are shown in Figure 12. The control system is quite robust to modeling errors and again results in a smooth steady state transition. Finally, the production rate was increased by 5%. This is achieved by introducing a step change of 1–1.05 in $u_{v,6}$. The corresponding responses of the process variables are shown in Figure 13. The proposed control scheme enables smooth transition in this case too, demonstrating its flexibility to demand changes.

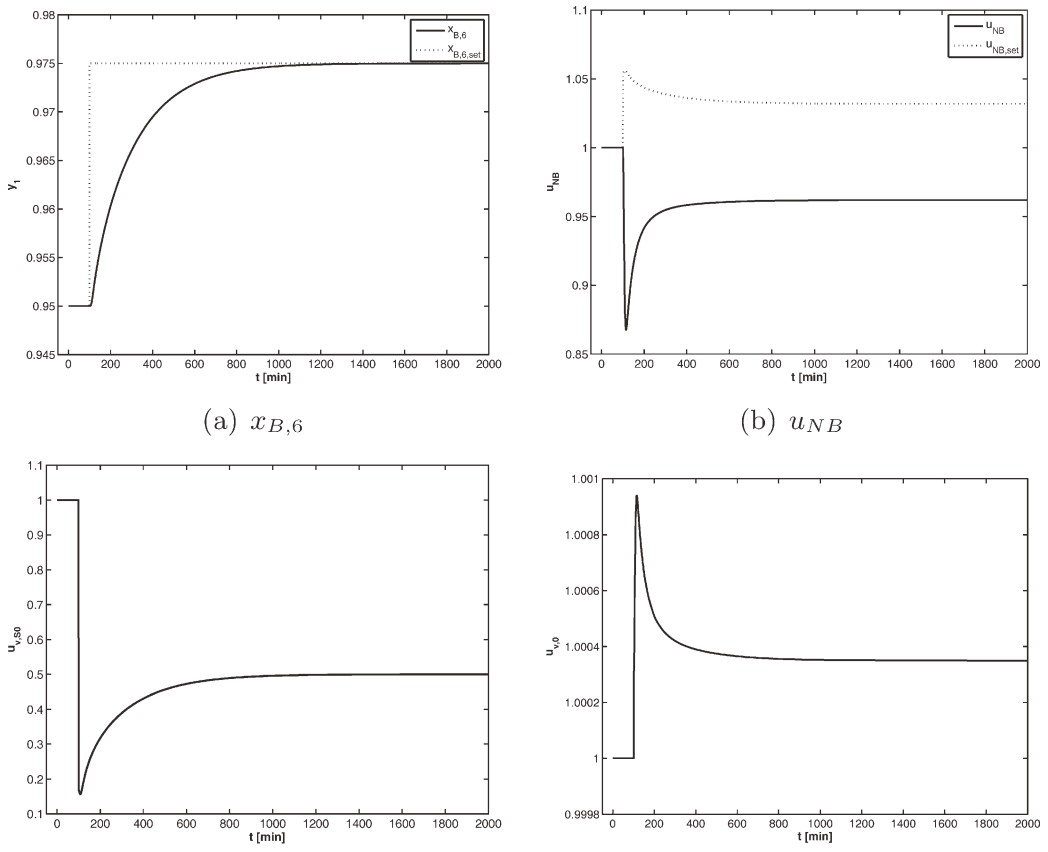

(a) $x_{B,6}$ (b) u_{NB}

(c) u_{S0} (d) u_0

Figure 11. Closed loop response of the biphasic system for a set point change in product purity.

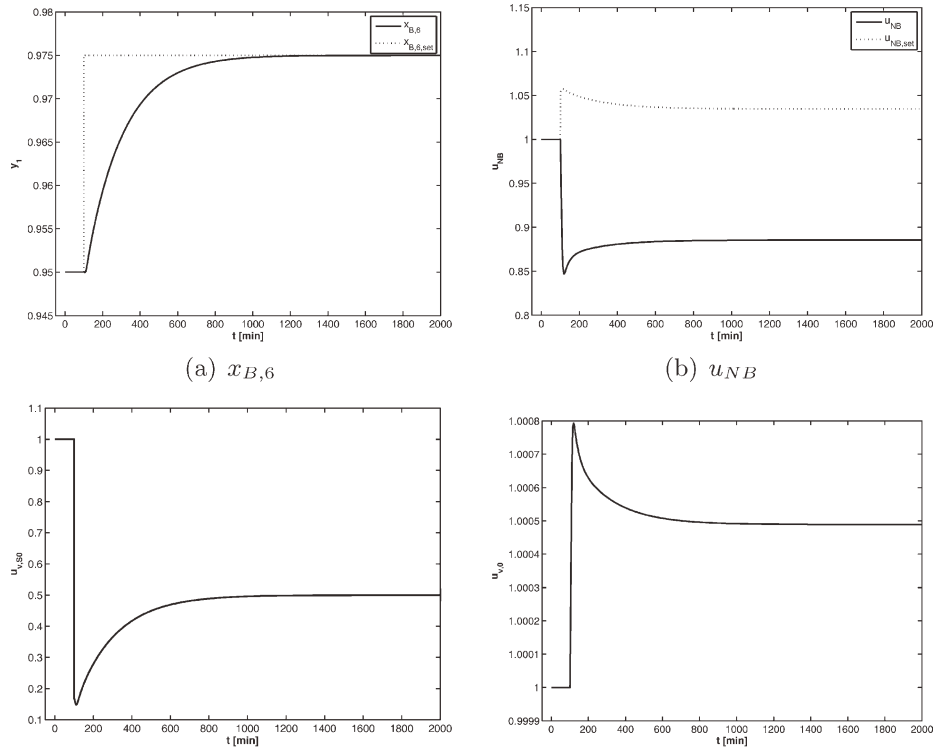

(a) $x_{B,6}$ (b) u_{NB}

(c) u_{S0} (d) u_0

Figure 12. Closed loop response of the biphasic system for a set point change in product purity, in the presence of modeling errors.

Note that if the full model (Eq. 17) along with the holdup controllers (Eq. 18) is used for the derivation of an input/output linearizing controller for y_1, it can be verified that the relative degree for y_1 is 2. This supports the claim in Remark 5 that the relative degree for x_N ($x_{B,6}$ in this case) could be different for the full and the reduced order model.

Remark 6 *In all the simulation scenarios, it can be noted that the fast controller does not reach the set point requested*

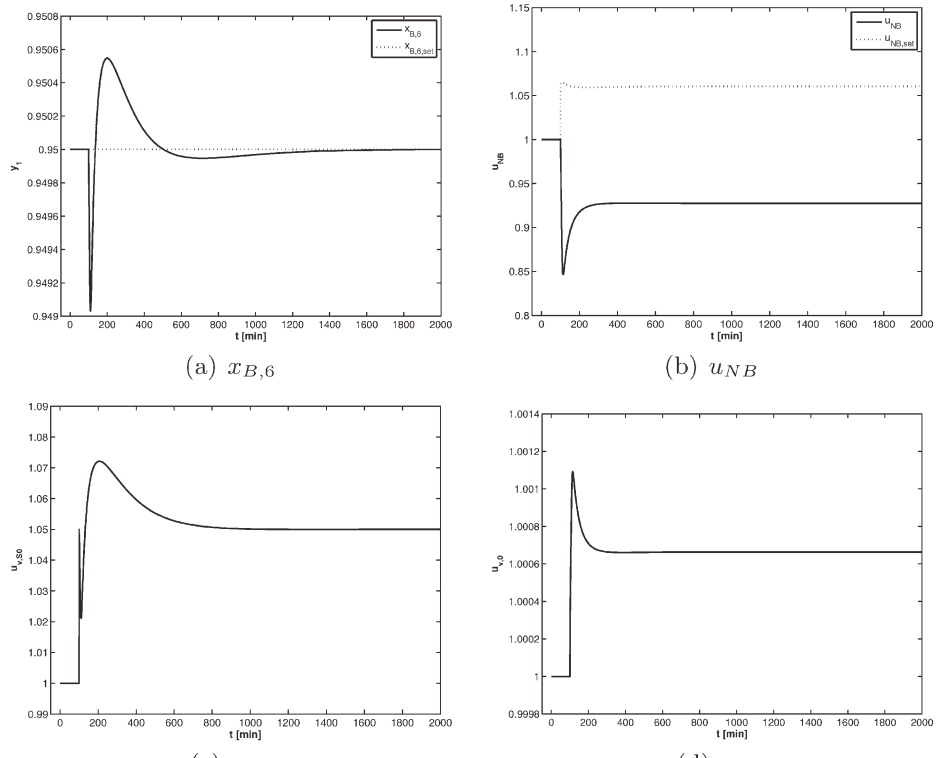

(a) $x_{B,6}$ (b) u_{NB}

(c) u_{S0} (d) u_0

Figure 13. Closed loop response of the biphasic system for an increase in the production rate.

by the slow controller (given the absence of any integral action). However, the product purity set point is still achieved. The slow model-based controller assumes that there is no deviation in the mass transfer rate across the liquid–liquid extractor ($u_{NEB} = 1$). *However, manipulation of* $v_{v,0}$ *via the fast controller (Eq. 19) introduces deviations in* u_{NEB}. *These deviations are not incorporated in the calculation of* $u_{NB,set}$. *The external integral action in (Eq. 20) ensures that the product purity set point is reached by compensating for all these mismatches (fast controller offset,* $u_{NEB} \neq 1$ *and controller-dynamic model mismatch*).

Concluding Remarks

In this article, a systematic framework for the analysis and control of process networks featuring large solvent recycle was developed. Such networks are very common, particularly in bio-based processes (for extracting a valuable chemical) and wastewater treatment (for removing impurities). A prototype network capturing the essential features of such networks was proposed. This network was shown to exhibit two time-scale dynamics, with the individual process units evolving at a faster rate compared to the network. Motivated by this time scale separation, a hierarchical control strategy was proposed to achieve key control objectives in each time scale. The proposed framework was applied to a relevant biorefinery example of HMF production from fructose. The proposed control strategy yielded excellent transitions in product quality and quantity, and demonstrated robustness to modeling errors.

Acknowledgments

Partial financial support for this work by the National Science Foundation grants CBET-0756363 and CBET-0855863, and University of Minnesota Doctoral Dissertation Fellowship for S.S.J. is gratefully acknowledged.

Notation

d = flowrate, mol s^{-1}
F = flowrate, mol s^{-1}
k = $\mathcal{O}(1)$ steady state ratio
K = controller gain
M = holdup, mol
N_B = mass transfer rate across the reactor, mol s^{-1}
N_{EB} = mass transfer rate across the extractor, mol s^{-1}
u = $\mathcal{O}(1)$ scaled flow
v = flowrate, mol min^{-1}
x = mol fraction
y = controller output

Greek letters

β = nonlinear controller tuning parameter
ε = singular perturbation parameter
κ = partition coefficient
$\aleph$ = kinetic rate constant min^{-1}
ρ = density, mol m^{-3}
τ = stretched time scale, s

Subscripts

A = fructose
B = HMF
BPA = byproducts of fructose
BPB = byproducts of HMF
Ev = evaporator
Ex, aq = extractor aqueous phase
Ex, org = extractor organic phase
r = reaction
R = recycle
R, aq = reactor aqueous phase
R, org = reactor organic phase
s = steady state value
set = set point value
W = water

Literature Cited

1. Zaks A, Klibanov AM. Enzyme-catalyzed processes in organic solvents. *Proc Natl Acad Sci USA*. 1985;82:3192–3196.
2. Kobayashi S. Recent developments in lipase-catalyzed synthesis of polyesters. *Macromol Rapid Commun*. 2009;30:237–266.
3. Adams JP, Collis AJ, Henderson RK, Sutton, PW. *Biotransformations in Small-molecule Pharmaceutical Development*. In: Whittall J, Sutton P. editors. *Practical Methods for Biocatalysis and Biotransformations*. Chichester: Wiley, 2009:1–82.
4. Illanes A. *Enzyme Biocatalysis: Principles and Applications*. Dordrecht: Springer, 2008.
5. Wheeler C, West KN, Liotta CL, Eckert CA. Ionic liquids as catalytic green solvents for nucleophilic displacement reactions. *Chem Commun*. 2001;37:887–888.
6. van Rantwijk F, Madeira Lau R, Sheldon RA. Biocatalytic transformations in ionic liquids. *Trends Biotechnol*. 2003;21:131–138.
7. Yang Z, Pan W. Ionic liquids green solvents for nonaqueous biocatalysis. *Enzyme Microb Technol*. 2005;37:19–28.
8. Sureshkumar M, Lee CK. Biocatalytic reactions in hydrophobic ionic liquids. *J Mol Catal B-Enzym*. 2009;60:1–12.
9. Sutlknot T, Hlmmelstel KJ. Desorption of phenol from activated carbon by solvent regeneration. *Ind Eng Chem Fundam.* 1983;22: 420–425.
10. Guo D, Shi Q, He B, Yuan X. Different solvents for the regeneration of the exhausted activated carbon used in the treatment of coking wastewater. *J Hazard Mater*. 2011;186:1788–1793.
11. Dye SR, Ng KM. Bypassing eutectics with extractive crystallization: Design alternatives and tradeoffs. *AIChE J*. 1995;41:1456–1470.
12. Roman-Leshkov Y, Chheda J, Dumesic J. Phase modifiers promote efficient production of hydroxymethylfurfural from fructose *Science* 2006;312:1933–1937.
13. Olsson G, Newell B. *Wastewater Treatment Systems: Modeling, Diagnosis and Control*. International Water Association, London: IWA Publishing, 1999.
14. Grassi VG. *Process design and control of extractive distillation*. In: Luyben WL. *Practical Distillation Control*. New York: Van Norstrand Reinhold, 1992.
15. Luyben WL. Plantwide control of an isopropyl alcohol dehydration process. *AIChE J*. 2006;52:2290–2296.
16. Luyben WL. Effect of solvent on controllability in extractive distillation. *Ind Eng Chem Res*. 2008;47:4425–4439.
17. Baldea M, Daoutidis P. Control of integrated process networks. A multi-time-scale perspective. *Comput Chem Eng*. 2007;31:426–444.
18. Jillson KR, Ydstie BE. Process networks with decentralized inventory and flow control. *J Process Contr*. 2007;17:399–413.
19. Sun Y, El-Farra NH. Quasi-decentralized model-based networked control of process systems. *Comput Chem Eng*. 2008;32:2016–2029.
20. Liu J, de la Peña DM, Ohran BJ, Christofides PD, Davis JF. A two-tier architecture for networked process control. *Chem Eng Sci*. 2008;63:5394–5409.
21. Sun Y, El-Farra NH. A quasi-decentralized approach for networked state estimation and control of process systems. *Ind Eng Chem Res*. 2010;49:7957–7971.
22. Kumar A, Daoutidis P. Nonlinear dynamics and control of process systems with recycle. *J Process Control*. 2002;12:475–484.
23. Baldea M, Daoutidis P. Modeling, dynamics and control of process networks with high energy throughput. *Comput. Chem. Eng*. 2008;32:1964–1983.
24. Jogwar SS, Baldea M, Daoutidis P. Dynamics and control of process networks with large energy recycle. *Ind. Eng. Chem. Res*. 2009;48: 6087–6097.
25. Jogwar SS, Baldea M, Daoutidis P. Tight energy integration: dynamic impact and control challenges. *Comput. Chem. Eng*. 2010; 34:1457–1466.
26. Kumar A, Christofides PD, Daoutidis P. Singular perturbation modeling of nonlinear processes with nonexplicit time-scale multiplicity. *Chem Eng Sci*. 1998;53:1491–1504.
27. Daoutidis P, Kravaris C. Dynamic output feedback control of minimum-phase multivariable nonlinear processes. *Chem Eng Sci*. 1994; 49:433–447.
28. Christofides PD, Daoutidis P. Feedback control of two-time-scale nonlinear systems. *Int. J. Control* 1996;63:965–994.
29. Kumar A, Daoutidis P. Structural analysis and output feedback control of nonlinear multivariable processes. *AIChE J*. 1994;40:647–669.

30. Kuster B, Temmink H. The influence of pH and weak-acid anions on the dehydration of D-fructose. *Carbohyd Res*. 1977;54:185–191.
31. Torres AI, Daoutidis P, Tsapatsis M. Continuous production of 5-hydroxymethylfurfural from fructose: a design case study. *Energy Environ Sci*. 2010;3:1560–1572.
32. Kumar A, Daoutidis P. *Control of Nonlinear Differential Algebraic Equation Systems: With Application to Chemical Processes*. Boca Raton: Chapman & Hall/CRC, 1999.

Manuscript received Feb. 9, 2011, and revision received May 4, 2011.